

Helicobacter pylori VacA Disrupts Apical Membrane-Cytoskeletal Interactions in Gastric Parietal Cells*[§]

Received for publication, January 22, 2008, and in revised form, June 18, 2008. Published, JBC Papers in Press, July 14, 2008, DOI 10.1074/jbc.M800527200

Fengsong Wang^{‡§}, Peng Xia[§], Fang Wu[§], Dongmei Wang[§], Wei Wang[¶], Tarsha Ward[‡], Ya Liu[‡], Felix Aikhionbare[‡], Zhen Guo^{‡§}, Michael Powell[‡], Bingya Liu^{||}, Feng Bi^{**}, Andrew Shaw[‡], Zhenggang Zhu^{||}, Adel Elmoselhi[‡], Daiming Fan^{‡‡}, Timothy L. Cover^{§§}, Xia Ding^{¶¶1}, and Xuebiao Yao^{§§2}

From the [§]Division of Cellular Dynamics, University of Science and Technology of China and Hefei National Laboratory for Physical Sciences at Nanoscale, Hefei 230027, China, [¶]Beijing University of Chinese Medicine, Beijing 100029, China, [‡]Morehouse School of Medicine, Atlanta, Georgia 30310, ^{**}Department of Abdominal Cancer, West China Hospital, Sichuan University, Chengdu 610041, China, ^{‡‡}Key Laboratory of Cancer Biology, Fourth Military Medical University, Xi'an, Shanxi 710032, China, ^{§§}Departments of Medicine and Microbiology and Immunology, Vanderbilt University School of Medicine, and Veterans Affairs Tennessee Valley Healthcare System, Nashville, Tennessee 37232, and ^{||}Institute of Digestive Surgery, Shanghai Jiaotong University, Shanghai 210026, China

Helicobacter pylori persistently colonize the human stomach and have been linked to atrophic gastritis and gastric carcinoma. Although it is well known that *H. pylori* infection can result in hypochlorhydria, the molecular mechanisms underlying this phenomenon remain poorly understood. Here we show that VacA permeabilizes the apical membrane of gastric parietal cells and induces hypochlorhydria. The functional consequences of VacA infection on parietal cell physiology were studied using freshly isolated rabbit gastric glands and cultured parietal cells. Secretory activity of parietal cells was judged by an aminopyrine uptake assay and confocal microscopic examination. VacA permeabilization induces an influx of extracellular calcium, followed by activation of calpain and subsequent proteolysis of ezrin at Met⁴⁶⁹–Thr⁴⁷⁰, which results in the liberation of ezrin from the apical membrane of the parietal cells. VacA treatment inhibits acid secretion by preventing the recruitment of H,K-ATPase-containing tubulovesicles to the apical membrane of gastric parietal cells. Electron microscopic examination revealed that VacA treatment disrupts the radial arrangement of actin filaments in apical microvilli due to the loss of ezrin integrity in parietal cells. Significantly, expression of calpain-resistant ezrin restored the functional activity of parietal cells in the presence of VacA. Proteolysis of ezrin in VacA-infected parietal cells is a novel mechanism underlying *H. pylori*-induced inhibition of acid secretion. Our results indicate that VacA disrupts

the apical membrane-cytoskeletal interactions in gastric parietal cells and thereby causes hypochlorhydria.

Helicobacter pylori are Gram-negative bacteria that colonize the gastric mucosa in more than half of the world's human population and persist despite a vigorous host immune response. Infection with these organisms consistently results in gastric inflammation and is a risk factor for the development of peptic ulcer disease, distal gastric adenocarcinoma, and gastric lymphoma (1, 2). Some individuals who are persistently infected with *H. pylori* develop a body-predominant atrophic gastritis and profound suppression of gastric acid secretion (3, 4). Atrophic gastritis is considered a risk factor for the development of gastric adenocarcinoma (5). In addition to causing hypochlorhydria in the setting of chronic infection, *H. pylori* also can cause hypochlorhydria in the setting of acute infection (6). The molecular mechanisms underlying *H. pylori*-induced hypochlorhydria have remained incompletely understood.

Acid secretion by the gastric parietal cell is regulated by paracrine, endocrine, and neural pathways. The physiological stimuli for acid secretion include histamine, acetylcholine, and gastrin, each of which binds to receptors located on the basolateral plasma membranes. Stimulation of acid secretion typically involves an activation of a cAMP-dependent protein kinase cascade that triggers the translocation and insertion of the proton pump enzyme, H,K-ATPase, into the apical plasma membrane of parietal cells (7). Ezrin is an actin-binding protein of the ezrin/radixin/moesin family of cytoskeleton-membrane linker proteins (8, 9) and, within the gastric epithelium, has been localized exclusively to parietal cells and primarily to the apical canalicular membrane of these cells (10). Our previous studies show that gastric ezrin is co-distributed with the β -actin isoform *in vivo* (11) and preferentially binds to the β -actin isoform *in vitro* (9). Based on the cytolocalization and observed stimulation-dependent phosphorylation of ezrin, it was postulated that ezrin couples the activation of protein kinase A to the apical membrane remodeling associated with parietal cell secretion (10, 12). Indeed, we have recently mapped the protein kinase A phosphorylation site on ezrin and elucidated the phosphoregulation of gastric acid secretion (13).

* This work was supported, in whole or in part, by National Institutes of Health Grants DK56292, CA89019, CA132389, AI39657, DK53623, and G-12-RR03034. This work was also supported by Chinese Academy of Science Grants KSCX1-YW-R65 and KSCX2-YW-H-10; Chinese 973 project Grants 2002CB713700, 2007CB914503, and 2006CB943603; Chinese Natural Science Foundation Grants 30270654, 39925018, 30500183, and 30570926; Chinese 863 Project Grants 2001AA215331 and 2006AA02A247; Chinese Minister of Education Grant 200203580851 (to X. Y.); 111 Project 07007 (to X. D.); and the Department of Veterans Affairs. The costs of publication of this article were defrayed in part by the payment of page charges. This article must therefore be hereby marked "advertisement" in accordance with 18 U.S.C. Section 1734 solely to indicate this fact.

[§] The on-line version of this article (available at <http://www.jbc.org>) contains supplemental Table S1 and Figs. S1–S3.

¹ To whom correspondence may be addressed. E-mail: xding@bucm.edu.cn.

² An American Digestive Health Foundation Research Scholar and a Georgia Cancer Coalition Eminent Cancer Scholar. To whom correspondence may be addressed. E-mail: yaoxb@ustc.edu.cn.

One mechanism by which *H. pylori* infection may inhibit gastric acid secretion is by stimulating production of the proinflammatory cytokine interleukin 1 β , which is known to be a potent inhibitor of gastric acid secretion (14). Another plausible hypothesis is that a secreted *H. pylori* factor may directly target parietal cells and alter parietal cell physiology. One of the major proteins secreted by *H. pylori* is an 88-kDa toxin, VacA, which exerts a variety of effects on epithelial cells *in vitro*, including the formation of large intracellular vacuoles, formation of anion-selective pores in the plasma membrane, apoptosis, and epithelial monolayer permeabilization (15–17). Studies in animal models, as well as epidemiologic studies of *H. pylori* isolates from humans, have suggested that VacA enhances the ability of *H. pylori* to colonize the stomach and also contributes to the development of symptomatic diseases (15). When isolated from *H. pylori* broth cultures, purified VacA is in an oligomeric state consisting predominantly of dodecameric or tetradecameric flower-shaped structures (18, 19). These oligomeric forms of VacA are relatively inactive (19). However, exposure of purified VacA to acidic or alkaline pH conditions results in disassembly of VacA oligomers into monomeric subunits, which can permeabilize target cell membranes (19). Upon binding to the target cell membrane, VacA can insert into the plasma membrane to form anion-selective pores/channels (20). Internalization of VacA into host cells or expression of the VacA protein in host cells results in the formation of intracellular vacuoles and alterations in intracellular membrane dynamics (21, 22).

In the current study, we tested the hypothesis that *H. pylori* VacA can alter gastric parietal cell physiology. We demonstrate that the VacA toxin acts directly on gastric parietal cells and induces an influx of extracellular calcium. The elevation of intracellular calcium induces hypochlorhydria via activation of calpain in parietal cells. These findings provide a novel mechanistic link between *H. pylori* infection and perturbation of parietal cell physiology.

MATERIALS AND METHODS

Purification of *H. pylori* VacA—VacA was purified in an oligomeric form from culture supernatant of *H. pylori* strain 60190 (American Type Culture Collection, Manassas, VA), as described previously (19). In most experiments, purified VacA was acid-activated by the slow addition of 200 mM HCl to the toxin preparation until a pH of 3.0 was reached (19). Such an acid activation was required to permeabilize parietal cells. In some experiments, VacA was heat-inactivated by boiling at 95 °C for 2 min.

DNA Construction—GFP²-ezrin was constructed by ligating an EcoRI-SalI PCR-amplified ezrin cDNA into pEGFP-N1 (Clontech), as described previously (13). The GFP-ezrin^{V466G} and histidine-ezrin^{V466G} mutants were constructed by a standard PCR method as described previously (13), and all plasmids were sequenced in full.

Antibodies—Ezrin antibody 4A5 was produced and described by Hanzel *et al.* (23). Actin antibody was purchased from Sigma. Rhodamine-coupled phalloidin and AlexFluor 350-conjugated goat anti-rabbit IgG were purchased from Invitrogen. Anti-VacA rabbit serum 958 was used at a 1:1,500 dilution (24).

Isolation of Gastric Glands and Parietal Cell Culture—Gastric glands were isolated from New Zealand White rabbits as modified by Yao *et al.* (25). To test whether VacA toxin permeabilization causes ezrin breakdown, treated gastric glandular cells were harvested and solubilized in SDS-PAGE sample buffer, as described previously (25). Equal amounts of total proteins were loaded for Western blot analysis. Isolation of gastric parietal cells and primary cultures of gastric parietal cells from rabbit stomach were produced and maintained as previously described (26).

VacA Permeabilization of Gastric Glands and Cultured Parietal Cells—Purified VacA was stored in aliquots at –80 °C. Reconstituted VacA solutions were kept on ice until use. Aliquots of gastric glands were pretreated with different doses (μ g/ml) of active VacA for 5 min followed by stimulation with histamine plus isobutylmethylxanthine (IBMX) in the presence of 1.8 mM calcium.

In some cases (for VacA washout experiments), intact glands in HEPES-minimal essential medium were washed two times by settling at 4 °C in ice-cold K buffer (10 mM Tris base, 20 mM HEPES acid, 100 mM KCl, 20 mM NaCl, 1.2 mM MgSO₄, 1 mM NaH₂PO₄, and 40 mM mannitol, pH 7.4). VacA was added to the glands (at 5% cytocrit) and then incubated on ice until the glands had completely settled (10–15 min). The K buffer supernatant containing excess VacA was removed, and the glands were washed two more times by settling at 4 °C in ice-cold K buffer. Finally, glands were resuspended in K buffer solution containing 1 mM pyruvate, 10 mM succinate, 1.8 mM calcium and then incubated at 37 °C for 3 min to allow the VacA pores to form. VacA-treated glands were used immediately or maintained on ice until use.

Immunofluorescence and Confocal Microscopy—For cytochemicalization of ezrin, F-actin, and H,K-ATPase, some cultures were treated with 100 μ M cimetidine to maintain a resting state; others were treated with the secretory stimulants 100 μ M histamine plus 50 μ M IBMX (26). Treated cells were then fixed with 4% formaldehyde and washed with phosphate-buffered saline, followed by permeabilization in 0.1% Triton X-100 for 5 min. Ezrin was labeled by a fluorescein isothiocyanate-conjugated goat anti-mouse antibody and counterstained with rhodamine-coupled phalloidin to visualize filamentous actin. Coverslips were supported on slides by grease pencil markings and mounted in Vectashield (Vector). Images were taken on a Zeiss Axiovert 200 fluorescence microscope using a 63 \times 1.3 numerical aperture PlanApo objective. Figures were constructed using Adobe Photoshop.

Immunostained parietal cells were examined under a laser-scanning confocal microscope LSM510 NLO (Carl Zeiss) scan head mounted transversely to an inverted microscope (Axiovert 200; Carl Zeiss) with a 40 \times 1.0 numerical aperture PlanApo objective. Single images were collected by an averaging of 10 scans at a scan rate of 1 s/scan. Optical section series were

² The abbreviations used are: GFP, green fluorescent protein; IBMX, isobutylmethylxanthine; BAPTA-AM, 1,2-bis(2-aminophenoxy)ethane-*N,N,N',N'*-tetraacetic acid acetoxyethyl ester; AP, aminopyrine.

H. pylori VacA Induces Hypochlorhydria

collected with a spacing of 0.4 μm in the z axis through the $\sim 12\text{-}\mu\text{m}$ thickness of the cultured parietal cells. The images from triple labeling were simultaneously collected using a dichroic filter set with Zeiss image processing software (LSM 5; Carl Zeiss). Digital data were exported into Adobe Photoshop for presentation.

In Vitro Ezrin Proteolysis by Calpain I—Recombinant histidine-ezrin was generated and purified using nickel beads as described previously (27). Equivalent amounts of ezrin proteins (50 μg) were incubated with 50 ng of purified calpain I (Calbiochem) at 25 °C for 5 min according to the instruction manual. The reaction was quenched by adding 4 \times SDS-PAGE sample buffer and boiled at 95 °C for 2 min. Following separation on 6–16% gradient SDS-PAGE, ezrin proteins were either transblotted onto a polyvinylidene difluoride membrane for microsequencing or stained with Coomassie Blue. The stained bands were then removed for mass spectrometric analysis as described (28).

^{14}C -Labeled Aminopyrine Uptake Assays—Stimulation of intact or VacA-treated gastric glands was quantified using the aminopyrine (AP) uptake assay, essentially as previously described (29). For both intact and permeabilized preparations, glands were kept in the resting state with cimetidine (10 μM). Intact preparations were stimulated with 50 μM IBMX and 100 μM histamine. Permeabilized preparations were stimulated with 100 μM cAMP plus 1 mM ATP. Other drugs used in selected experiments included the H,K-ATPase-specific proton pump inhibitor 5 μM SCH-28080 (30) and the protein kinase A inhibitor 10 μM H89 (29). Gland preparations were incubated for 20 min at 37 °C with shaking (~ 160 oscillation/min) with or without various reagents as specified and then centrifuged briefly to pellet the glands. The pellets were dried and weighed, and aliquots of both the supernatant and pellet were counted in a Beckman liquid scintillation counter. These data were used to calculate the AP accumulation ratio (ratio of intracellular to extracellular AP concentration). To normalize AP uptake values among the various preparations, the data from some experiments are expressed as a fraction of the stimulated control.

Measurement of Parietal Cell $[\text{Ca}^{2+}]_i$ in Response to VacA Treatment—To examine if VacA increases intracellular calcium level in parietal cells, we have carried out intracellular calcium ($[\text{Ca}^{2+}]_i$) measurement in isolated gastric glandular cell population. In addition, we planned for a preliminary throughput assay to learn the relative change in $[\text{Ca}^{2+}]_i$ produced by VacA treatments in a variety of different conditions. For those reasons, measurement of $[\text{Ca}^{2+}]_i$ was done using a modification of a 96-well fluorescence assay, as previously described (31). Isolated gastric glands were loaded with 2.5 μM Fluo 4-AM for 45 min at 37 °C. After being loaded, the glands were washed twice with mammalian Ringer solution and then incubated with different concentrations of VacA for $[\text{Ca}^{2+}]_i$ measurement in fresh Ringer solution at 37 °C. In some experiments, VacA was washed out after incubation with gastric glands, for 3 min on ice, prior to $[\text{Ca}^{2+}]_i$ measurement. Fluo 4 fluorescence was recorded using a 96-well fluorescence plate reader (FluoStar; BMG Technologies, Durham, NC) equipped with excitation (485 \pm 20-nm) and emission (530 \pm 20-nm)

filters. A treatment of heat-inactivated VacA was included as a control. In another set of experiments, gastric glands preloaded with Fluo 4 were treated with 1 μM calpain inhibitor E64d or 1 mM calcium chelator BAPTA-AM for 5 min at 37 °C before incubation with active VacA for $[\text{Ca}^{2+}]_i$ measurement. In general, fluorescence measurements were made every 5 s after incubation with VacA. The F_{max} measurement for the human gastric epithelial cells was obtained by adding a solution of 5 μM ionomycin and 100 μM digitonin to the gastric cells for 15 min. After this, the F_{min} measurement was obtained by adding a solution of 10 mM EGTA, 10 mM EDTA in 60 mM Tris-HCl, pH 10.5, for 15 min. The values for F_{max} and F_{min} were graphed, and individual fluorescence values were obtained by using a single wavelength equation for Fluo 4 (32). The calibration calcium concentration curve was generated by using a series of defined Ca^{2+} calibration solutions (Molecular Probes), and $[\text{Ca}^{2+}]_i$ was calculated.

Analyses of Ezrin Integrity in VacA-infected Human Biopsies—Biopsy samples were taken from the antrum and corpus of 30 subjects undergoing routine endoscopic and histologic examination for dyspeptic symptoms. From each biopsy site, part of the samples was used for PCR-based VacA characterization (32), and part was solubilized in SDS-PAGE sample buffer for Western blot analyses. Twenty-one cases were *H. pylori*-positive, and nine were negative based upon light microscopy investigation. Among the 21 positive samples, 13 were VacA-positive.

Electron Microscopy—Isolated gastric glands were treated with acid-activated or boiled VacA prior to histamine stimulation. These treated glands were then fixed in 2% glutaraldehyde (Tousimis) in phosphate-buffered saline and processed as previously described (9, 34). Thin serial sections (silver-gold) were then cut, poststained, and examined with a JEOL 1200 electron microscope (Peabody, MA).

Western Blotting Analyses—Samples were subjected to SDS-PAGE on a 6–16% gradient gel and transferred onto nitrocellulose membrane. Proteins were probed by appropriate primary antibodies and detected using ECL (Pierce). The band intensity was then quantified using a PhosphorImager (Amersham Biosciences).

RESULTS

***H. pylori* VacA Inhibits Acid Secretion from Gastric Glands**—To directly assess whether *H. pylori* VacA perturbs parietal cell acid secretion, we incubated isolated gastric glands with VacA and measured acid secretion, using an aminopyrine (AP) uptake assay. The addition of boiled VacA caused relatively small changes in AP uptake (at most, a $\sim 6\%$ decrease), and there was no dose-dependent inhibitory effect (Fig. 1A). In contrast, acid-activated VacA caused a dose-dependent inhibition of acid secretion in isolated glands, as measured by AP uptake. No significant inhibitory effect was noted in experiments with 0.1 $\mu\text{g}/\text{ml}$ VacA, but 1 $\mu\text{g}/\text{ml}$ VacA caused a 22.1% reduction in acid secretion, and 5–10 $\mu\text{g}/\text{ml}$ VacA caused a 76–85% reduction. Preincubation of VacA with an anti-VacA antibody prior to its incubation with gastric glands abolished the VacA effect on acid secretion (data not shown). These experiments sug-

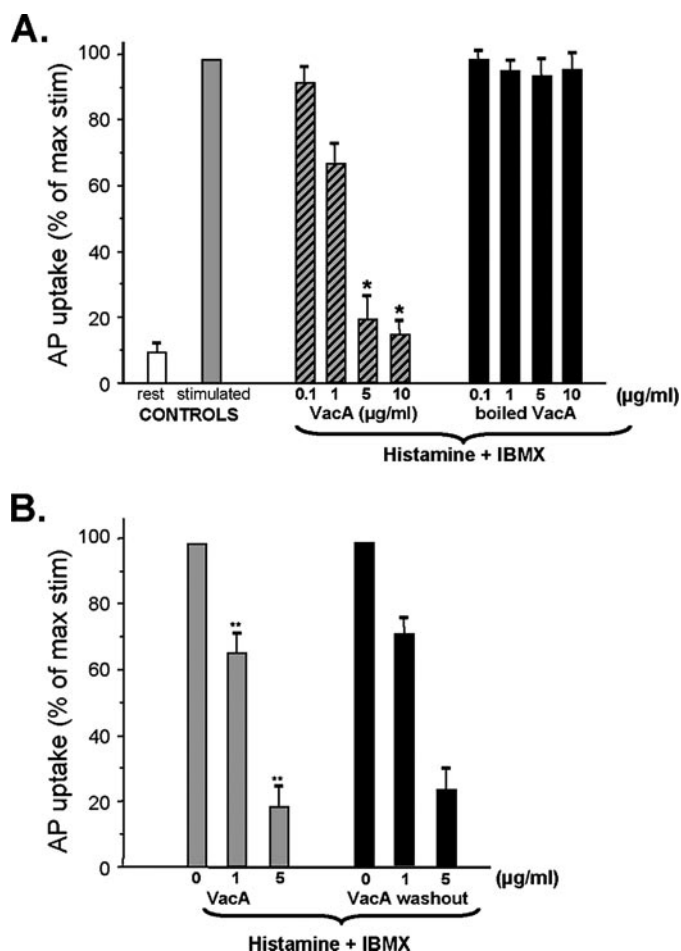


FIGURE 1. *H. pylori* VacA toxin inhibits acid secretion from gastric glands. *A*, intact glands were kept in the resting state with cimetidine (*Rest*) or stimulated with histamine plus IBMX in the presence of 1.8 mM calcium (*stimulated*; $n = 10$). Aliquots of gastric glands were pretreated with different doses ($\mu\text{g/ml}$) of acid-activated VacA or inactive (boiled) VacA for 5 min, followed by stimulation with histamine plus IBMX for additional 20 min in the presence of 1.8 mM calcium. *Error bars*, S.E. ($n = 6$). The AP uptake ratios are expressed as a fraction of the stimulated control. *B*, aliquots of gastric glands were pretreated with different doses ($\mu\text{g/ml}$) of active VacA for 5 min followed by stimulation with histamine plus IBMX in the presence of 1.8 mM calcium; alternatively, unbound VacA was removed prior to the stimulation (*washout*). *Error bars*, S.E. ($n = 5$). The AP uptake ratios are expressed as a fraction of the stimulated control. Note that inhibition of acid secretion does not require the presence of VacA during the stimulation.

gested that the VacA toxin inhibits parietal cell acid secretion in isolated gastric glands.

In an effort to minimize VacA internalization into cells, we also used a modified protocol that included a step in which glands were incubated with VacA at 4 °C. After washout of unbound VacA, the AP uptake assay was initiated by warming glands at 37 °C in the presence of histamine and IBMX. The permeability of glandular cells was judged by the labeling of the actin cytoskeleton using rhodamine-conjugated phalloidin. VacA-induced permeabilization occurred rapidly (within 3 min) when the glands were warmed to 37 °C. About $\sim 93 \pm 3\%$ of VacA-treated glandular cells were labeled with rhodamine phalloidin, regardless which protocol was used (with or without washout of unbound VacA). In contrast, only $6 \pm 1\%$ of the control cells (not treated with VacA) were stained with rhodamine-phalloidin (data not shown). As shown in Fig. 1*B*, both

protocols resulted in a similar inhibition of AP uptake. These experiments suggest that VacA-induced permeabilization of the plasma membrane results in inhibition of parietal cell secretion.

VacA Inhibits Gastric Acid Secretion via Mobilization of Intracellular Calcium—VacA forms pores/channels in the plasma membrane of host cells (20), and *H. pylori* treatment can induce cytosolic calcium oscillations in gastric epithelial cells (21, 36). Activation of the calcium-dependent proteinase calpain I results in an inhibition of acid secretion in parietal cells (25); therefore, we sought to test whether the inhibition of acid secretion by VacA is mediated by an influx of extracellular calcium. As shown in Fig. 2*A*, titrating extracellular calcium with EGTA or pretreatment of cells with BAPTA-AM, an intracellular calcium chelator (20), effectively attenuated the VacA-induced inhibition of parietal cell acid secretion, judged by the AP uptake assay. This suggests that an influx of calcium from the extracellular pool contributes to the inhibition of acid secretion in VacA-treated gastric glands. In support of this view, when glands were treated with activated VacA in the absence of extracellular calcium, no inhibition of acid secretion was detected (data not shown), and no inhibition was detected in the presence of extracellular magnesium (supplemental Fig. 3).

If VacA-induced calcium mobilization activates calpain I, resulting in an inhibition of parietal cell secretion, inhibition of calpain activation would be expected to antagonize the VacA-induced inhibition of acid secretion. Indeed, if glands were pretreated with the calpain I inhibitor E64d, VacA had no inhibitory effect on acid secretion (Fig. 2*B*). In contrast, if the glands were pretreated with the serine protease inhibitor PafBloc as a control, VacA blocked acid secretion. These studies suggest that the calcium-dependent protease calpain I is activated in VacA-treated glands, which results in an inhibition of parietal cell acid secretion.

Our previous studies showed that activation of calpain I results in liberation of ezrin from the apical and canalicular membranes of parietal cells (37, 38). To examine whether VacA induces delocalization of ezrin, we performed immunostaining of ezrin. In control gastric glands treated with boiled VacA, ezrin was localized in typical apical and canalicular sites of the parietal cells (Fig. 2*C*, *a*; *arrows*). However, VacA treatment resulted in fragmentation of gastric glands and liberation of ezrin from the apical and canalicular membrane; as a result, the cells displayed a diffuse cytoplasmic staining (Fig. 2*C*, *b*; *arrows*). If this relocation of ezrin is mediated by an elevation of intracellular calcium, blocking the increase in intracellular calcium should prevent the relocation of ezrin from the membrane to the cytoplasm. Indeed, when gastric glands were pretreated with intracellular calcium chelator BAPTA-AM before incubation with VacA, ezrin remained localized to apical and canalicular membranes (Fig. 2*D*, *a*; *arrows*).

To examine if VacA treatment mobilizes intracellular calcium of gastric glandular cells, we carried out fluorescence measurement of Fluo 4-loaded gastric glandular cells in response to VacA treatment. Our trial time course experiment revealed that VacA treatment produces a typical biphasic $[\text{Ca}^{2+}]_i$ increase with a peak followed by a plateau, which is seen

H. pylori VacA Induces Hypochlorhydria

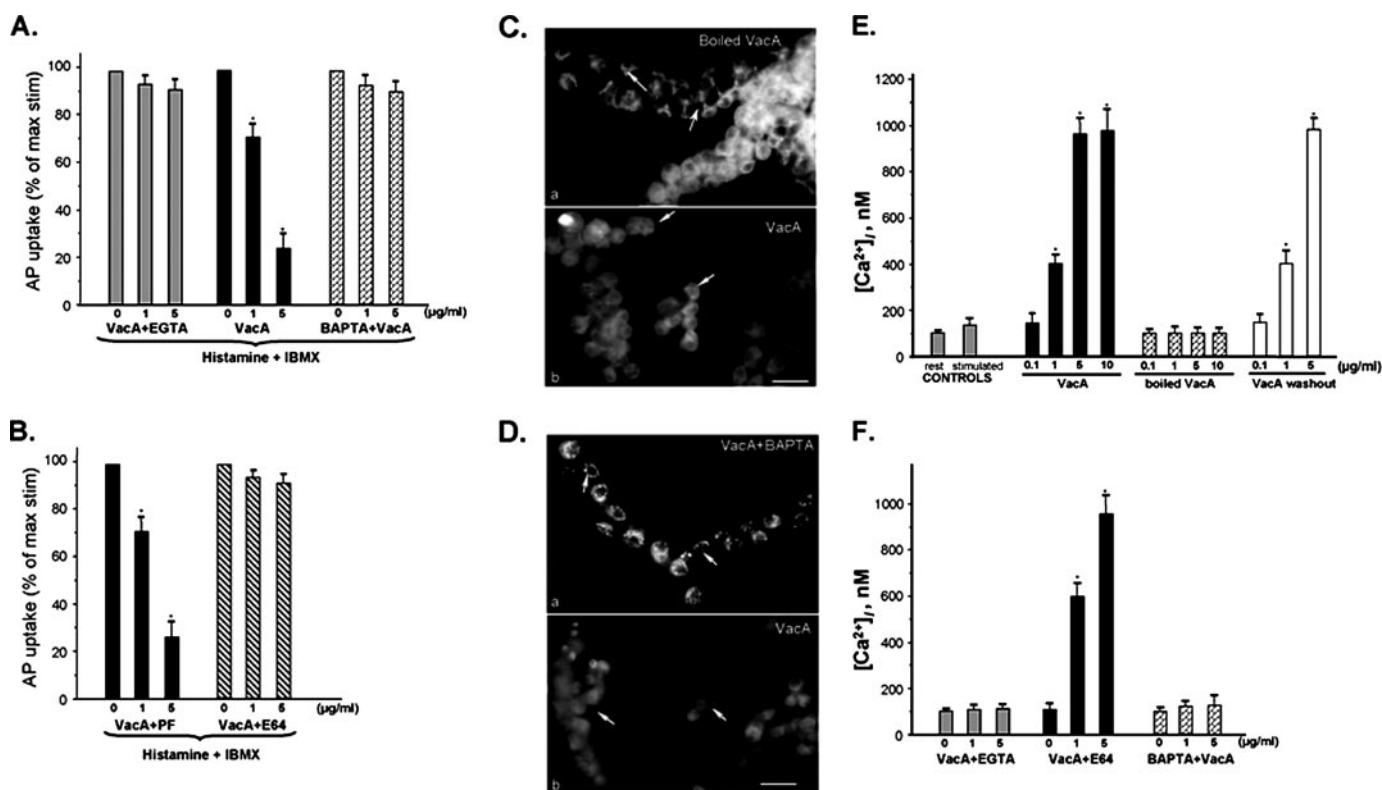


FIGURE 2. VacA-induced inhibition of acid secretion is mediated by calcium influx. *A*, aliquots of gastric glands were pretreated with different concentrations ($\mu\text{g/ml}$) of active VacA for 5 min in the presence of 2 mM EGTA plus 1.8 mM Ca^{2+} , 1.8 mM Ca^{2+} , or 1 mM BAPTA-AM plus 1.8 mM Ca^{2+} , followed by stimulation with histamine + IBMX for 20 min. Error bars, S.E. ($n = 6$). The AP uptake ratios are expressed as a fraction of the stimulated control. *B*, aliquots of gastric glands were pretreated with the protease inhibitor E64d or Pafblocc (PF) in the presence of VacA ($\mu\text{g/ml}$) for 5 min followed by stimulation with histamine plus IBMX in calcium-containing medium (1.8 mM Ca^{2+}). Error bars, S.E. ($n = 4$). The AP uptake ratios are expressed as a fraction of the stimulated control. *C*, aliquots of gastric glands were pretreated with active or inactive (boiled) VacA (5 $\mu\text{g/ml}$) for 20 min in the presence of 1.8 mM Ca^{2+} followed by fixation and staining for ezrin. In glands treated with boiled VacA, ezrin was specifically located to the apical membrane of parietal cells (*a*; arrows) but not other epithelial cells in gastric glands. In glands treated with active VacA, the glands were dispersed, and ezrin was no longer localized in an apical site (*b*; arrows). *D*, aliquots of gastric glands were pretreated with 1 mM BAPTA-AM for 5 min before incubation with active VacA (5 $\mu\text{g/ml}$) for 20 min in the presence of 1.8 mM Ca^{2+} . The gastric glands were then fixed and stained for ezrin. In glands pretreated with BAPTA-AM, ezrin is located to the apical membrane of parietal cells (*a*; arrows). However, ezrin became dispersed in glands not pretreated with BAPTA before incubation with VacA (*b*; arrows). *E*, effects of VacA treatment on $[\text{Ca}^{2+}]_i$ changes in isolated rabbit gastric glands. The gastric glands were loaded with Fluo 4 prior to treatment with secretagogues, VacA toxin, or heat-inactivated VacA, in the presence of 1.8 mM extracellular calcium. In some cases, VacA toxin was incubated with gastric glands for 3 min on ice prior to $[\text{Ca}^{2+}]_i$ recording. Compared with cimetidine-treated glands, Histamine stimulation resulted in a brief elevation of $[\text{Ca}^{2+}]_i$. VacA treatment results in a dose-dependent increase of peak $[\text{Ca}^{2+}]_i$, which is also seen in VacA washout experiments. Heat-inactivated VacA failed to mobilize $[\text{Ca}^{2+}]_i$. Data are from five independent experiments and expressed as means \pm S.E.; $p < 0.05$ versus peak levels of heat-inactivated VacA treatments. *F*, effects of calcium chelators on VacA-induced $[\text{Ca}^{2+}]_i$ changes in isolated rabbit gastric glands. The gastric glands were loaded Fluo 4 prior to treatment with VacA toxin. Aliquots of gastric glands were pretreated with calpain inhibitor E64d or calcium chelator BAPTA-AM as described under "Materials and Methods." In some cases, 2 mM EGTA was added into the Ringer solution prior to $[\text{Ca}^{2+}]_i$ measurements. Both calcium chelators EGTA and BAPTA-AM minimized the VacA-induced $[\text{Ca}^{2+}]_i$ mobilization. Treatment of calpain inhibitor E64d did not modulate the effect of VacA on mobilization of $[\text{Ca}^{2+}]_i$. Data are from five independent experiments and expressed as means \pm S.E.; $p < 0.05$ versus peak levels of heat-inactivated VacA treatment.

in *H. pylori*-induced $[\text{Ca}^{2+}]_i$ in gastric mucous cells (31). The transient peak $[\text{Ca}^{2+}]_i$ typically appears 7 min after the VacA treatment. As shown in Fig. 2*E*, VacA treatment caused a dose-dependent increase in peak $[\text{Ca}^{2+}]_i$. At the highest VacA concentration used (10 $\mu\text{g/ml}$), there was a change in $[\text{Ca}^{2+}]_i$ from a basal level of 102 ± 9 nM (e.g. cimetidine-treated samples without VacA) to a peak of 973 ± 103 nM ($n = 6$; $p < 0.05$) in the presence of 1.8 mM extracellular calcium. This response was also observed in isolated parietal cells or primary parietal cell culture (data not shown). This dose-dependent response was not seen in gastric glandular cells treated with heat-inactivated VacA. As predicted, VacA washout after initial incubation of VacA with gastric glands did not alter the profile of VacA-induced mobilization of $[\text{Ca}^{2+}]_i$ (Fig. 2*E*, right).

To ascertain if the mobilization of $[\text{Ca}^{2+}]_i$ is a result of calcium influx from extracellular medium, we chelated extracellular

calcium with 2 mM EGTA. As predicted, chelating extracellular calcium abolished the VacA-induced dose-dependent increase in $[\text{Ca}^{2+}]_i$ (Fig. 2*F*). Similarly, pretreatment of gastric glandular cells with BAPTA-AM also prevented the mobilization of $[\text{Ca}^{2+}]_i$. On the other hand, the addition of calpain inhibitor E64d did not cause the alteration of $[\text{Ca}^{2+}]_i$ (Fig. 2*F*). Thus, we conclude that VacA-induced inhibition of parietal cell acid secretion is mediated by a calcium influx and depletion of ezrin from the apical and canalicular membrane.

VacA-induced Mobilization of Intracellular Calcium Activates Calpain I, Which Hydrolyzes Ezrin—Our previous studies showed that activation of calpain I in gastric parietal cells results in liberation of ezrin from the apical membrane and hydrolysis of ezrin (25). The hydrolysis of ezrin yields a typical 55-kDa breakdown product recognized by monoclonal antibody 6H11 (23, 25). If calpain I is activated by VacA toxin, VacA

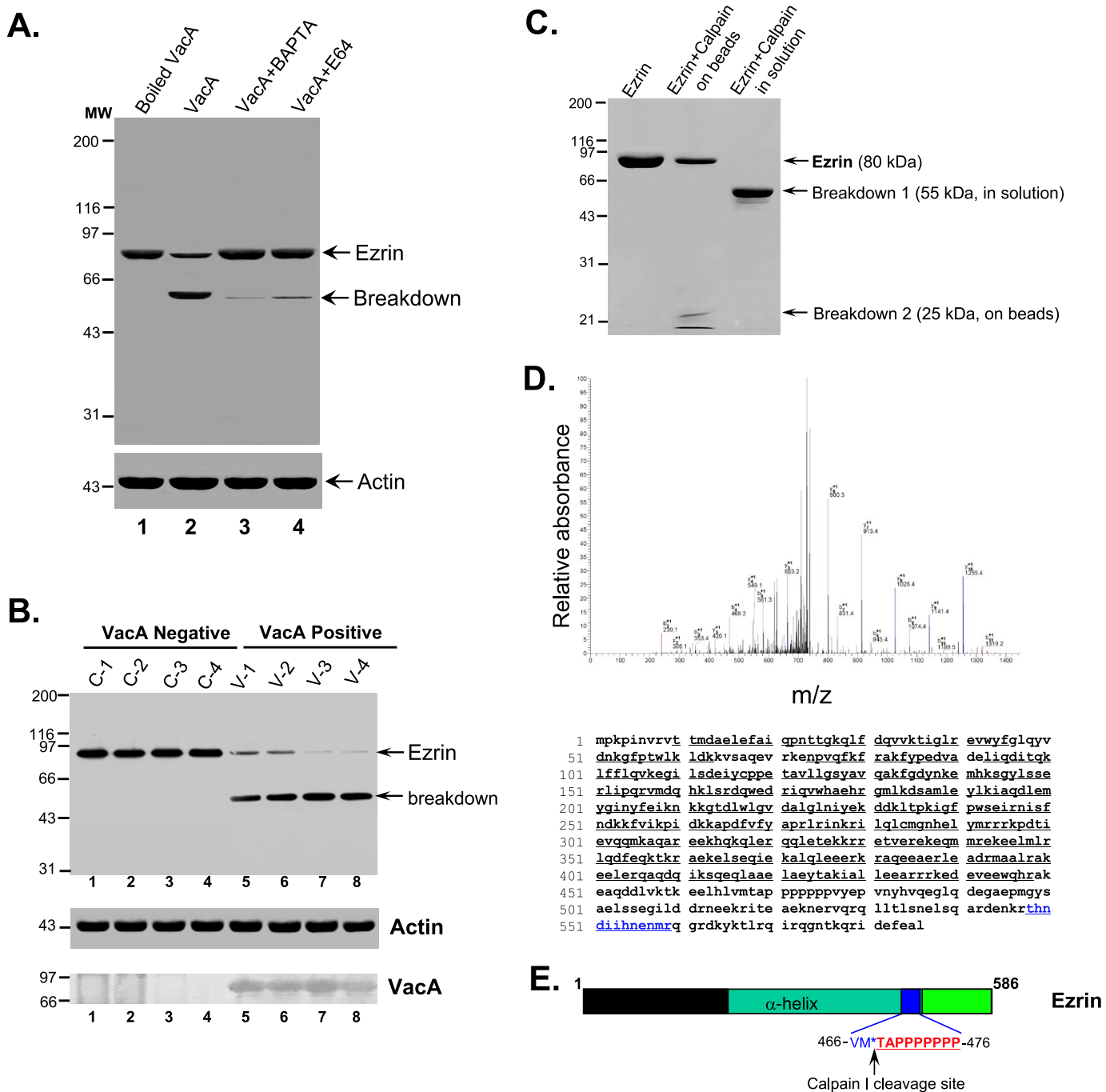


FIGURE 3. VacA treatment induces a Ca²⁺-dependent cleavage of ezrin at Met⁴⁶⁹-Thr⁴⁷⁰. A, aliquots of gastric glands were pretreated with E64d, BAPTA-AM, or vehicle for 5 min, followed by incubation with VacA (5 μg/ml) for 20 min in the presence of 1.8 mM Ca²⁺. An aliquot of glands was treated with boiled VacA. Glandular cells were then collected and solubilized in SDS-PAGE sample buffer. Equivalent amounts of proteins from these gland samples were applied to SDS-PAGE and subsequently transblotted onto nitrocellulose membrane. The blot was probed for ezrin and actin using an ECL kit (Pierce). B, ezrin is hydrolyzed in VacA-infected human biopsies from dyspeptic patients. An aliquot of human gastric biopsies from VacA-positive patients (V1–V4) and negative control patients (C1–C4) were homogenized in SDS-PAGE sample buffer. Equivalent amounts of proteins from these gland samples were applied to SDS-PAGE and subsequently transblotted onto nitrocellulose membrane. The blot was probed for ezrin (top), actin (middle), and VacA (bottom) using an ECL kit (Pierce). Note that hydrolysis of ezrin from an intact 80 kDa band to a typical calpain-cleaved 55 kDa band seen only in VacA-positive biopsies (lanes 5–8) correlated with the presence of VacA from those biopsies (lanes 5–8). C, histidine-tagged ezrin proteins were expressed in bacteria and purified using nickel-agarose beads as described under “Materials and Methods.” Equivalent amounts of ezrin proteins (50 μg) were incubated with 0.1 μg of purified calpain I at 25 °C for 5 min, followed by separation on 6–16% gradient SDS-PAGE and staining with Coomassie Blue. The visualized proteins included ezrin, a 55-kDa breakdown product, and a 25-kDa breakdown product. The 55 and 25 kDa protein bands were excised for in-gel digestion and subsequent mass spectrometric analyses (D). Ezrin proteins from a duplicate SDS-polyacrylamide gel were transblotted onto polyvinylidene difluoride membrane, and the 25 kDa band was microsequenced (E). D, representative liquid chromatography-tandem mass spectrometry spectra of a tryptic fragment derived from the 25-kDa breakdown product of ezrin (THNDIIHNEMR) (top) and highlighted peptide sequence (bottom). E, schematic diagram of microsequencing results (sequencing data are listed in Fig. S1).

H. pylori VacA Induces Hypochlorhydria

treatment of cells should result in proteolysis of ezrin, and either inhibition of calpain I or blocking of calcium influx into cells would be expected to block the hydrolysis of ezrin. Consistent with this hypothesis, Western blot analysis demonstrated that VacA treatment induced hydrolysis of ezrin and yielded a typical 55-kDa hydrolytic product (Fig. 3A, lane 2). Pretreatment of glands with BAPTA-AM and the calpain inhibitor E64d blocked the ezrin breakdown. The addition of E64d (a calpain I inhibitor) effectively inhibits ezrin hydrolysis, which is consistent with the reported median inhibitory concentration (IC₅₀) values for this inhibitor (38). This calpain-mediated proteolysis appears specific for ezrin, since Western blot analyses revealed no alteration in actin, tubulin, or PALS1 in VacA-treated samples. These results indicate that the VacA toxin induces calpain I-mediated selective cleavage of ezrin *in situ*.

If *H. pylori* VacA targets directly to gastric parietal cell in humans, ezrin would be hydrolyzed from VacA-positive biopsies from dyspeptic patients. To test this hypothesis, samples from patient biopsies with dyspeptic symptoms were collected for analysis of ezrin integrity. As shown in Fig. 3B, Western blot analysis demonstrated that a typical calpain-mediated hydrolysis of ezrin, judged by the 55-kDa hydrolytic product (breakdown), was readily apparent in VacA-positive (lanes 5–8) but not VacA-negative biopsies (lanes 1–4). The 80-kDa ezrin is relatively intact in biopsies from VacA-negative biopsies (lanes 1–4). Western blot analysis of VacA confirmed the correlation between ezrin breakdown and presence of VacA (Fig. 3B, *bottom*), suggesting that the gastric parietal cell is a direct target of VacA toxin in dyspeptic patients and that ezrin breakdown is an outcome of VacA-positive human biopsies.

To verify that calpain I directly hydrolyzes ezrin, we incubated a carboxyl-terminal histidine-tagged recombinant ezrin immobilized on nickel beads with purified calpain I. The addition of 1 μM Ca²⁺ efficiently stimulated the cleavage of ezrin and generated a 55-kDa cleavage product liberated from nickel beads (Fig. 3C, lane 3). Furthermore, this cleavage product was recognized by the ezrin monoclonal antibody 4A5; the epitope recognized by this antibody resides in the amino terminus of the ezrin molecule. To characterize this 55-kDa product generated from the amino terminus of ezrin, we excised the 55 kDa band from the SDS-PAGE gel and performed an in-gel digestion with trypsin. The tryptic peptides were analyzed using liquid chromatography-tandem mass spectrometry. As listed in Table S1, 36 peptides (e.g. VTTMAELEFAIQPNTTGK, IAQDLEMYGINIFYEIK, PKEDEVEEWQHR, and AKEAQD-DLVK) were identified as tryptic fragments of the amino-terminal 55-kDa fragment of ezrin (amino acids 9–458). In addition, mass spectrometric analysis of the 25-kDa proteolytic fragment bound to nickel beads revealed three peptides (e.g. ITEAEKNER, QLLTLSSLSQAR, and THNDIIHNENMR), confirming that this 25-kDa proteolytic fragment is derived from the carboxyl terminus of ezrin. The mass spectrum of the tryptic peptide THNDIIHNENMR is shown in Fig. 3D. To determine the calpain I cleavage site, we microsequenced the 25 kDa protein band transferred onto polyvinylidene difluoride membrane. The seven amino acids from the N terminus of this fragment are TAPPPPP and are located near the polyproline sequence of ezrin (Fig. 3E; also see Fig. 1). Together, these

experiments indicate that VacA-induced calcium influx and activation of calpain I result in hydrolysis of ezrin and inhibition of acid secretion in gastric glands.

VacA Toxin-induced Inhibition of Acid Secretion Is a Direct Result of Ezrin Hydrolysis in Gastric Parietal Cells—A recent ultrastructural study demonstrated that *H. pylori* infects and penetrates into gastric epithelial cells from luminal sides (39). If the VacA toxin-induced inhibition of acid secretion in gastric glands is a function of ezrin breakdown, treatment of isolated parietal cells with VacA toxin should mimic the inhibitory response seen in the isolated gastric glands. Rabbit parietal cells establish an interesting morphology in culture. Within a few h of plating onto Matrigel, parietal cells appear to lose their polarity by engulfing the apical canalicular membranes into a series of vacuolar inclusions (e.g. see Ref. 30). When parietal cells at rest (nonsecreting) are stained with phalloidin, F-actin is primarily localized to the apical vacuoles and to the basolateral membrane. Analogous to its staining pattern *in situ* (23), ezrin is distributed as a subset of F-actin, largely localized to the apical vacuoles and, to a lesser extent, the basolateral membrane, whereas H,K-ATPase is distributed throughout the cytoplasm (e.g. see Ref. 13).

To prevent the internalization of VacA into cells and prevent possible VacA-induced effects on the activity of secretory organelles, we incubated VacA (5 $\mu\text{g}/\text{ml}$) with cultured parietal cells on ice for 3 min, followed by washout of unbound VacA prior to a 20-min incubation at 37 °C in the absence of extracellular calcium. VacA-bound parietal cells were fixed, permeabilized, and stained for VacA, ezrin, and F-actin. As shown in Fig. 4A (resting cells), ezrin is mainly located at the apical plasma membrane of parietal cells (seen as *green rings*) in a pattern suggestive of the apical plasma membrane invaginations that form the intracellular canaliculi (Fig. 4A, *a*). Labeling of F-actin mainly outlines the apical plasma membrane of parietal cells in a pattern similar to that of ezrin (Fig. 4A, *b*; *red*) with less stain on the basolateral plasma membrane. Labeling of VacA with a rabbit antibody revealed that VacA is concentrated at the apical plasma membrane (Fig. 4A, *c*; *blue*). No basolateral localization of VacA was detected, and virtually no cytoplasmic labeling of VacA was observed in the parietal cells. Thus, we conclude that VacA is preferentially associated with the apical plasma membrane of parietal cells.

The correlation of VacA infection with the breakdown of ezrin propelled us to more directly investigate the impact of VacA treatment on parietal cell physiology. To this end, we treated cultured parietal cells with VacA toxin following the protocol described in Fig. 4A. Afterward, we assessed the ability of VacA-treated parietal cells to respond to histamine stimulation. In resting parietal cells treated with boiled VacA, ezrin outlines apical and canalicular membranes of gastric parietal cells (Fig. 4B, *a*). F-actin is mainly localized to the apical membrane of parietal cells, in a distribution similar to that of ezrin (Fig. 4B, *b*; *red*), whereas H,K-ATPase is localized in the cytoplasm and concentrated at the apical membrane vacuoles (Fig. 4B, *c*; *blue*). The stimulation of parietal cell acid secretion involves insertion of H,K-ATPase-containing tubulovesicle membranes into apical canalicular membranes, resulting in dilation of apical membrane vacuoles as active HCl and water

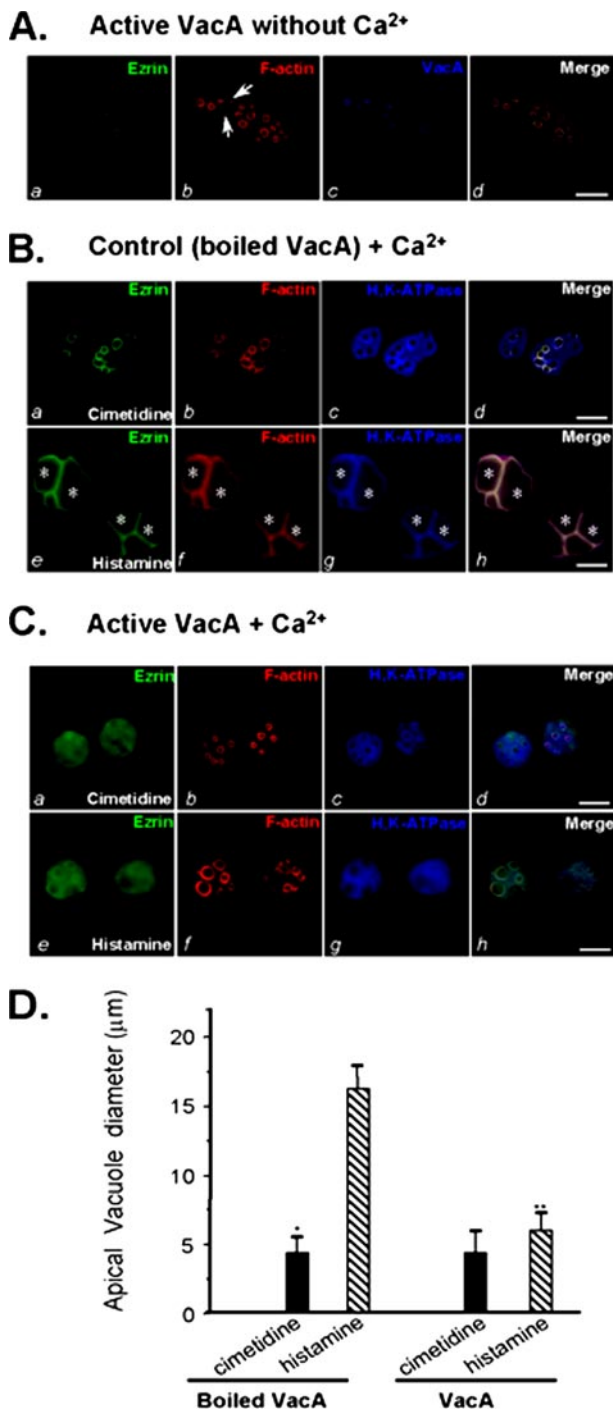


FIGURE 4. VacA-induced hydrolysis of ezrin results in an inhibition of acid secretion in cultured parietal cells. *A*, cultured parietal cells were incubated with VacA (5 µg/ml) on ice for 3 min, followed by washout of unbound VacA and warming at 37 °C for 20 min in the absence of extracellular calcium. The treated cells were fixed, permeabilized, and stained for ezrin, F-actin, and VacA. Ezrin marks the apical membrane of parietal cells (*a*), which is overlapped with the labeling of VacA (*d*). *Bar*, 10 µm. *B*, cultured parietal cells were incubated with inactive (boiled) VacA (5 µg/ml) in the presence of 1.8 mM Ca²⁺ for 5 min followed by a 20-min incubation with histamine or cimetidine. Treated cells were fixed and stained for ezrin, F-actin, and H,K-ATPase. *Bar*, 10 µm. *C*, cultured parietal cells were incubated with active VacA (5 µg/ml) for 5 min in the presence of 1.8 mM Ca²⁺ prior to a 20-min incubation with histamine or cimetidine. Treated cells were fixed and stained for ezrin, F-actin, and H,K-ATPase. *Bar*, 10 µm. *D*, cultured parietal cells were incubated with active VacA or inactive VacA for 20 min prior to stimulation with histamine plus IBMX. The diameters of apical vacuoles were measured as an index for apical membrane expansion associated with acid secretion. Data were obtained

transport occurs (13). In secreting cells pretreated with boiled VacA, the dilated apical canicular vacuoles occupy most of the cytoplasmic space, due to the recruitment of H,K-ATPase, as noted in our earlier studies (13). H,K-ATPase is redistributed to the dilated apical vacuole membrane (Fig. 4*B*, *g*; asterisks) and is superimposed with the distribution of ezrin and F-actin when the three images are merged (*h*; asterisks).

As predicted, treatment with active VacA in calcium-containing media results in liberation of ezrin from the apical plasma membrane of the parietal cells (Fig. 4*C*, *a*; green), which is reminiscent of what is seen in VacA-treated gastric glands (Fig. 2*C*, *b*). In contrast, F-actin remains localized to the apical plasma membrane, whereas the H,K-ATPase is localized to the cytoplasm (Fig. 4*C*, *b* and *c*). In the VacA-treated cells, histamine-stimulated H,K-ATPase relocation was not detected (Fig. 4*C*, *g*). Staining of F-actin confirmed that the apical vacuole membrane dilation is minimized in the VacA-treated parietal cells (Fig. 4*C*, *f*). Western blot analysis of ezrin validated the proteolysis of ezrin induced by VacA treatment (Fig. S2). Previous studies revealed that the diameter of vacuoles can be used as a reporter for parietal cell secretory activity (30). Thus, we surveyed ~50 cells from resting and stimulated populations treated with active and boiled VacA toxin proteins. Fig. 4*D* shows that stimulation dramatically increases the mean vacuole diameter to 16.3 ± 2.1 µm in parietal cells in the presence of inactive VacA (boiled VacA). However, the average vacuole diameter of VacA-treated, stimulated cells was only 5.7 ± 1.3 µm. Thus, VacA-induced hydrolysis of ezrin greatly attenuates secretion-dependent dilation of the vacuoles, suggesting that VacA-induced inhibition of acid secretion is a direct result of ezrin proteolysis in gastric parietal cells.

Prevention of Calpain-mediated Ezrin Hydrolysis Rescues VacA Toxin-induced Inhibition of Acid Secretion—If ezrin hydrolysis accounts for the attenuation of acid secretion in VacA-treated parietal cells, blocking ezrin hydrolysis should sustain the parietal cell secretion in the presence of VacA treatment. To this end, we mutated the calpain cleavage site and created a calpain-resistant ezrin^{V466G} based on its ability to resist proteolysis in the test tube (Fig. S3). Western blot analysis confirmed that the exogenously expressed GFP-ezrin^{V466G} protein remained intact, whereas the wild type GFP-ezrin was broken down in VacA-treated cultured parietal cells (Fig. 5*A*), demonstrating the ability of ezrin^{V466G} to protect against calpain cleavage in VacA-treated parietal cells. We next tested for the ability of ezrin^{V466G}-expressing cells to secrete acid in response to histamine stimulation. As shown in Fig. 5*B*, the dilated apical canicular vacuoles occupy most of the cytoplasmic space in ezrin^{V466G}-expressing secreting cells in the presence of VacA. H,K-ATPase is redistributed to the dilated apical vacuole membrane and is superimposed with the distribution of ezrin and F-actin when the three images are merged. In the wild type ezrin-expressing cells, histamine-stimulated H,K-

from resting and stimulated parietal cells in which apical vacuoles were in the same focal plane. These measurements were taken from four different preparations in which 75 cells from each category were examined. In resting cells, measurements were carried out on 2–5 vacuoles/cell, whereas 1–3 vacuoles/cell were analyzed in stimulated preparations. Data are expressed as means ± S.E.

H. pylori VacA Induces Hypochlorhydria

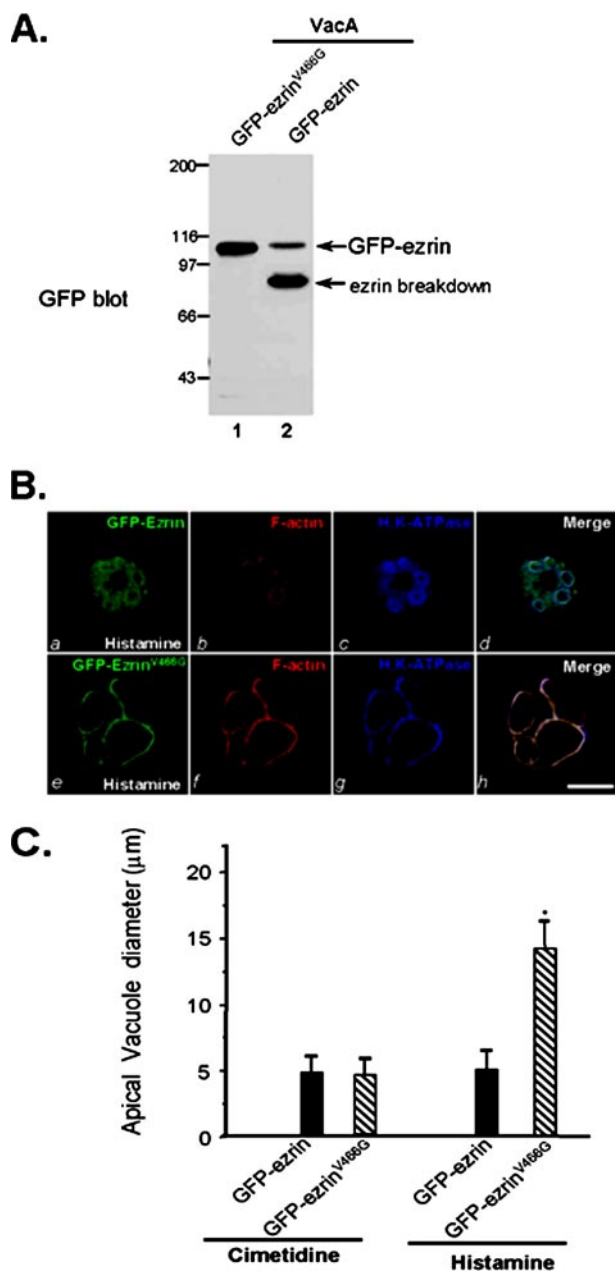


FIGURE 5. Block of calpain-mediated ezrin hydrolysis rescues VacA-induced inhibition of acid secretion. *A*, aliquots of cultured parietal cells transiently transfected to express wild type GFP-ezrin and GFP-ezrin^{V466G} mutant. Thirty-six hours after the transfection, the parietal cells were incubated with activated VacA (5 µg/ml) and boiled VacA in the presence of 1.8 mM Ca²⁺ for 20 min prior to being solubilized in SDS-PAGE sample buffer. Equivalent amounts of proteins from these samples were applied to SDS-PAGE and subsequently transblotted onto nitrocellulose membrane. The blot was probed with an anti-GFP antibody using an ECL kit (Pierce). Note that wild type GFP-ezrin but not GFP-ezrin^{V466G} is hydrolyzed in VacA-treated glandular cells. *B*, cultured parietal cells transiently transfected to express wild type GFP-ezrin and GFP-ezrin^{V466G} mutant. Thirty-six hours after the transfection, the parietal cells were incubated with activated VacA (10 µg/ml) and 100 mM histamine plus 50 mM IBMX in the presence of 1.8 mM Ca²⁺ for 20 min. Treated cells were fixed and stained for ezrin, F-actin, and H,K-ATPase. Note that the apical vacuoles are dilated in the GFP-ezrin^{V466G}-expressing cells but not wild type GFP-ezrin-expressing cells. *Bar*, 10 µm. *C*, 35 parietal cells positively expressing GFP-ezrin (wild type and ezrin^{V466G} mutant) and stimulated parietal cells were surveyed for apical vacuole diameters in the same focal plane as described in Fig. 4*D*. Data are expressed as means ± S.E.

ATPase relocation was not detected (Fig. 5*B*, *g*). Staining of F-actin confirms that the apical vacuole membrane dilation is minimized (Fig. 5*B*, *f*) and the apical distribution of ezrin is reduced (Fig. 5*B*, *e*), consistent with the observed proteolysis of wild type GFP-ezrin in VacA-treated cells (Fig. 5*A*, lane 1). A survey of 30 parietal cells expressing GFP-ezrin and GFP-ezrin^{V466G} from stimulated populations treated with VacA toxin shows that stimulation dramatically increases the mean vacuole diameter to 13.7 ± 3.1 µm in GFP-ezrin^{V466G}-expressing parietal cells exposed to VacA. However, the average vacuole diameter of VacA-treated, stimulated GFP-ezrin-expressing cells was only 5.3 ± 1.5 µm. The VacA-induced inhibition of parietal cell activation was restored in GFP-ezrin^{V466G}-expressing cells, validating that loss of ezrin results in VacA-induced inhibition of acid secretion in gastric parietal cells. Thus, we conclude that parietal cell physiology is directly altered by VacA toxin.

H. pylori VacA Disrupts the Apical Membrane-Cytoskeletal Cross-linking—Highly organized microfilaments are typical features of microvilli at the apical membrane within the parietal cell canaliculus. In going from a resting to the secreting state, there are major changes at the apical canalicular surface, including elongation of microvilli (12). If ezrin is the linker between the actin filaments and the apical plasma membrane in gastric parietal cells, *H. pylori* VacA-induced proteolysis of ezrin should disrupt the apical membrane-cytoskeletal interaction. To test this hypothesis, we carried out electron microscopic examination of gastric parietal cells treated with VacA, followed by histamine stimulation. A micrograph of the secreting parietal cell apical membrane is shown in Fig. 6*A*, and in this micrograph, elongated microvilli are readily apparent. The radial arrangement of the actin filaments in proximity to the plasma membrane is clearly seen in the *inset*. However, examination of VacA-treated parietal cells reveals that the radial arrangement of actin filaments was lost in the treated cells (Fig. 6*B*), indicating that VacA treatment disrupts the bridge between the radial actin filaments and the apical plasma membrane. We surveyed 120 cross-sections from 11 different cells that display a defined arrangement of actin filaments in both VacA-treated and control parietal cells. As shown in Fig. 6*C*, VacA treatment significantly increased the percentage of parietal cell apical microvilli exhibiting aberrant arrangement of actin filaments when viewed in the cross-section ($81 \pm 8\%$), whereas control preparation only exhibited a small fraction with aberrant arrangement ($9 \pm 2\%$; $p < 0.05$). The majority of the cross-section of control parietal cell microvilli contains a typical radial arrangement of actin bundles (Fig. 6*A*, *inset*). Thus, we conclude that *H. pylori* VacA toxin disrupts apical membrane-cytoskeletal interactions in parietal cells.

DISCUSSION

H. pylori infection results in gastric mucosal inflammation, termed chronic superficial gastritis, in all infected human subjects. In some *H. pylori*-infected persons, persistent infection can lead to the development of chronic atrophic gastritis, a condition characterized in part by diminished numbers of acid-producing parietal cells and reduced gastric acid secretion. Here, we provide the first evidence that *H. pylori* VacA toxin

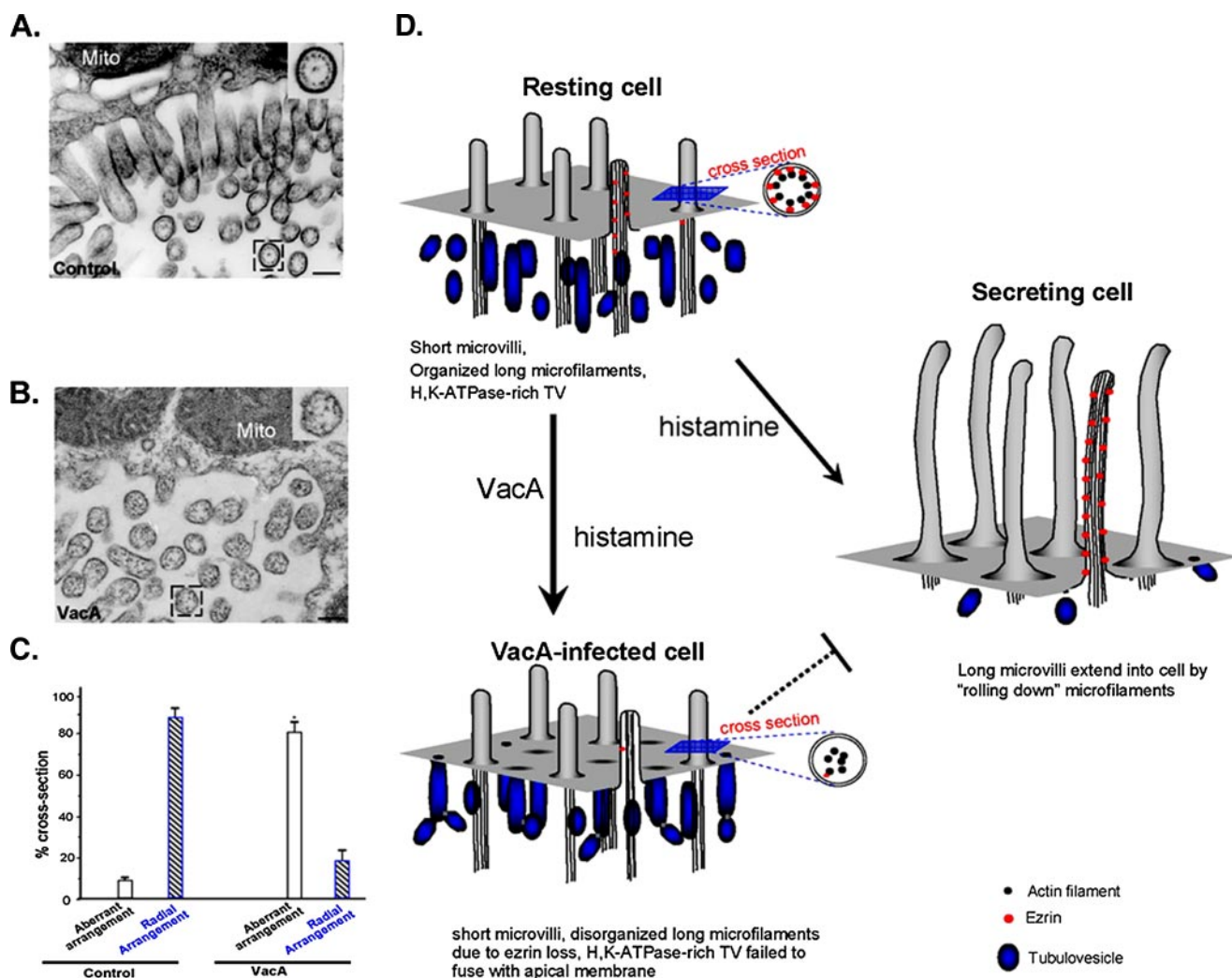


FIGURE 6. VacA-induced hydrolysis of ezrin disrupts the actin cytoskeleton-membrane association. *A*, microfilaments are highly organized in the apical microvilli of gastric parietal cells. Secreting gastric glands were processed as described under "Materials and Methods." Thin sections were poststained with uranyl acetate and lead citrate and examined under an electron microscope. In control secreting parietal cells, the greatly expanded apical membrane is lined with numerous elongated microvilli. A magnified view of a cross-section (*inset*) shows the radial arrangement of the actin filaments in proximity to the microvillar membrane in parietal cells. *B*, microfilaments-membrane association in parietal cell is disrupted by VacA treatment. VacA-treated secreting gastric glands were processed as described in *A*. In VacA-treated parietal cells, the apical membrane was lined with numerous short microvilli. A magnified view of a cross-section (*inset*) shows an aberrant arrangement of the actin filaments in the microvilli. *Bar*, 200 nm. *C*, statistics of actin filament arrangements seen in the cross-sections of parietal cell microvilli from both VacA-treated and control parietal cells. Values represent the means \pm S.E. of at least 120 microvillar cross-sections in 11 different cells. *D*, hypothetical scheme accounting for VacA-induced hypochlorhydria. In the resting cell, short, apical microvilli are supported by long microfilaments extending deep into the cytoplasm. Ezrin (red dot) links actin filaments with the apical plasma membrane. Stimulation leads to docking and fusion of H,K-ATPase-rich tubulovesicles to the apical plasma membrane, greatly expanding the apical surface. Interactions between the apical membrane and microfilaments, via ezrin, reorganize the expanded surface into long microvilli. However, VacA induces proteolysis of ezrin, which disrupts the interactions between the apical membrane and microfilaments, which prevents the recruitment of H,K-ATPase to the apical membrane. Defective recruitment of H,K-ATPase to the apical membrane results in hypochlorhydria in VacA-infected parietal cells.

impairs gastric parietal cell physiology by disrupting the apical membrane-cytoskeletal linker of gastric parietal cells. In addition, we further demonstrate that this disruption is mediated by calcium-dependent proteolysis of ezrin. The finding that ezrin hydrolysis in VacA-infected gastric biopsies together with the restoration of parietal cell physiology with calpain-resistant ezrin in VacA-infected cells argues for the relevance of ezrin hydrolysis in the disease states of *H. pylori* infection. Based on the results of the current study, we offer a working model accounting for a potential mechanism for *H. pylori*-induced hypochlorhydria (Fig. 6D).

A major role for the actin cytoskeleton in the secretory processes of parietal cells has been inferred from studies

using actin disruptors (40). Highly organized microfilaments are typical features of microvilli at the apical membrane within the parietal cell canaliculus. In going from the resting to the secreting state, there are major changes at the apical canalicular surface, including elongation of microvilli (12). Parietal cell activation involves translocation of H,K-ATPase from the cytoplasm to the apical plasma membrane via multiple steps, including possible trafficking over actin filaments, docking to secretory sites, insertion of the pump into the apical membrane, and perhaps maintenance of the pump in the apical membrane during active secretion (7). Our recent studies demonstrated that ezrin couples protein kinase A-mediated phosphorylation to the remodeling of the

H. pylori VacA Induces Hypochlorhydria

apical membrane cytoskeleton associated with acid secretion in parietal cells (13) and demonstrated H,K-ATPase trafficking to the plasma membrane (41). Tsukita and co-workers (42) recently showed the direct *in vivo* involvement of ezrin in gastric acid secretion by using a tissue-specific knockdown approach in mice. Suppression of ezrin expression (to <5% of wild type) resulted in a failure to remodel the apical and canalicular membrane and resulted in hypochlorhydria in mice (42). Although the ezrin-calpain I interactions in gastric parietal cells were discovered more than a decade ago (25), its biological relevance has remained elusive. The finding that calpain mediated hydrolysis of ezrin in VacA infection of parietal cells demonstrates a novel role of ezrin-calpain interaction in the pathogenesis of *H. pylori*-induced hypochlorhydria.

It has been shown that VacA can be internalized by human gastric epithelial cells into endosomal compartments via a Cdc42-dependent mechanism (43). Although Cdc42 is present at the apical membrane of parietal cells and is involved in acid secretion (26), we have been unable to find any obvious endosomal localization of VacA in our primary culture of parietal cells. Our studies show that a brief exposure of parietal cells to VacA results in permeabilization of the plasma membrane of the cells without interference of intracellular organelle membranes. In fact, VacA-permeabilized parietal cells, in the absence of calcium, are able to respond to cAMP-ATP stimulation in a manner similar to other permeabilization agents, such as α -toxin (Fig. S4). In this regard, the VacA-induced toxicity is mainly mediated by influx of extracellular calcium and subsequent activation of calpain, demonstrating that parietal cells are a novel target of *H. pylori* infection and associated hypochlorhydria.

H. pylori-induced gastritis is associated with a variety of clinical outcomes that include peptic ulcer disease (44) and gastric cancer (33). Patients with *H. pylori*-induced gastric ulcers or gastric cancer typically have corpus-predominant gastritis and low acid secretion due to functional inhibition of acid secretion (3, 4, 35). Gastric atrophy and hypochlorhydria are important and interdependent precursor abnormalities that significantly increase the risk of gastric cancer. It has been shown that *H. pylori*-induced proinflammatory factors, such as interleukin-1 β , can contribute to hypochlorhydria (4, 14), and certain polymorphisms in genetic determinants for interleukin-1 β have been linked to an increased risk for gastric cancer (4, 17). It is possible that inflammatory factors, such as interleukin-1 β , cause an inhibition of acid secretion from parietal cells via a paracrine pathway. Our finding that VacA acts directly on acid-secreting cells and induces hypochlorhydria via activation of calpain in parietal cells provides a novel mechanism for *H. pylori*-induced direct alterations in parietal cell physiology. It is worth noting that ezrin is broken down into 55-kDa fragments in gastric biopsies from *H. pylori*-infected patients but not in biopsies from *H. pylori*-negative patients (Fig. 3B). Since ezrin is an essential cytoskeletal component required for parietal cell plasticity and calpain I activation causes necrosis-mediated parietal cell loss (34), the VacA-induced ezrin breakdown may contribute to the loss of the parietal cell lineage that is characteristic of chronic atrophic gastritis. It would be of great interest

to test whether a combination of a calpain I inhibitor with the current *H. pylori* regimen would better the therapeutic outcome. Taken together, the outcomes presented in this work reveal that gastric parietal cells are directly targeted by VacA, resulting in calpain I-mediated hydrolysis of ezrin and inhibition of gastric acid secretion, mimicking the hypochlorhydric phenotype seen in *H. pylori*-infected patients.

Acknowledgments—We thank Dr. John Forte for insightful suggestions and Dr. Gordon Leitch for critical reading of the manuscript.

REFERENCES

1. Cover, T. L., Berg, D. E., Blaser, M. J., and Mobley, H. L. T. (2001) *Principles of Bacterial Pathogenesis* (Groisman, E. A., ed) pp. 510–558, Academic Press, Inc., San Diego, CA
2. Peek, R. M., and Blaser, M. J. (2002) *Nat. Rev. Cancer* **2**, 28–37
3. El-Omar, E. M., Oien, K., El-Nujumi, A., Gillen, D., Wirz, A., Dahill, S., Williams, C., Ardill, J. E., and McColl, K. E. (1997) *Gastroenterology* **113**, 15–24
4. Furuta, T., Baba, S., Takashima, M., Futami, H., Arai, H., Kajimura, M., Hanai, H., and Kaneko, E. (1998) *Scand. J. Gastroenterol.* **33**, 357–363
5. Correa, P. (1992) *Cancer Res.* **52**, 6735–6740
6. Morris, A., and Nicholson, G. (1987) *Am. J. Gastroenterol.* **82**, 192–199
7. Yao, X., and Forte, J. G. (2003) *Annu. Rev. Physiol.* **65**, 103–131
8. Bretscher, A., Edwards, K., and Fehon, R. G. (2002) *Nat. Rev. Mol. Cell Biol.* **3**, 586–599
9. Yao, X., Cheng, L., and Forte, J. G. (1996) *J. Biol. Chem.* **271**, 7224–7229
10. Urushidani, T., Hanzel, D. K., and Forte, J. G. (1999) *Am. J. Physiol.* **256**, G1070–G1081
11. Yao, X., Chaponnier, C., Gabbiani, G., and Forte, J. G. (1995) *Mol. Biol. Cell* **6**, 541–557
12. Forte, J. G., and Yao, X. (1996) *Trends Cell Biol.* **6**, 45–48
13. Zhou, R., Cao, X., Watson, C., Miao, Y., Guo, Z., Forte, J. G., and Yao, X. (2003) *J. Biol. Chem.* **278**, 35651–35659
14. Furuta, T., El-Omar, E. M., Xiao, F., Shirai, N., Takashima, M., and Sugimura, H. (2002) *Gastroenterology* **123**, 92–105
15. Cover, T. L., and Blanke, S. R. (2005) *Nat. Rev. Microbiol.* **3**, 320–332
16. de Bernard, M., Cappon, A., Del Giudice, G., Rappuoli, R., and Montecucco, C. (2004) *Int. J. Med. Microbiol.* **293**, 589–597
17. El-Omar, E. M., Carrington, M., Chow, W. H., McColl, K. E., Bream, J. H., Young, H. A., Herrera, J., Lissowska, J., Yuan, C. C., Rothman, N., Lanyon, G., Martin, M., Fraumeni, J. F., Jr., and Rabkin, C. S. (2002) *Nature* **404**, 398–402
18. Adrian, M., Cover, T. L., Dubochet, J., and Heuser, J. E. (2002) *J. Mol. Biol.* **318**, 121–133
19. Cover, T. L., Hanson, P. I., and Heuser, J. E. (1997) *J. Cell Biol.* **138**, 759–769
20. Szabo, I., Brutsche, S., Tombola, F., Moschioni, M., Satin, B., Telford, J. L., Rappuoli, R., Montecucco, C., Papini, E., and Zoratti, M. (1999) *EMBO J.* **18**, 5517–5527
21. de Bernard, M., Arico, B., Papini, E., Rizzuto, R., Grandi, G., Rappuoli, R., and Montecucco, C. (1997) *Mol. Microbiol.* **26**, 665–674
22. Ye, D., Willhite, D. C., and Blanke, S. R. (1999) *J. Biol. Chem.* **274**, 9277–9282
23. Hanzel, D. K., Urushidani, T., Usinger, W. R., Smolka, A., and Forte, J. G. (1989) *Am. J. Physiol.* **256**, G1082–G1089
24. Schraw, W., Li, Y., McClain, M. S., van der Goot, F. G., and Cover, T. L. (2002) *J. Biol. Chem.* **277**, 34642–34650
25. Yao, X., Thibodeau, A., and Forte, J. G. (1993) *Am. J. Physiol.* **265**, C36–C46
26. Zhou, R., Guo, Z., Watson, C., Chen, E., Kong, R., Wang, W., and Yao, X. (2004) *Mol. Biol. Cell* **14**, 1097–1108
27. Jin, C., Ge, L., Ding, X., Chen, Y., Wu, F., Cao, X., Wang, Q., and Yao, X. (2006) *Biochem. Biophys. Res. Commun.* **341**, 784–791
28. Fang, Z., Miao, Y., Ding, X., Deng, H., Liu, S., Wang, F., Zhou, R., Watson, C., Fu, C., Hu, Q., Lillard, J. W., Jr., Powell, M., Chen, Y., Forte, J. G., and

- Yao, X. (2006) *Mol. Cell Proteomics* **5**, 1437–1449
29. Ammar, D. A., Zhou, R., Forte, J. G., and Yao, X. (2002) *Am. J. Physiol.* **282**, G23–G33
30. Agnew, B. J., Duman, J. G., Watson, C. L., Coling, D. E., and Forte, J. G. (1999) *J. Cell Sci.* **112**, 2639–2646
31. Marlink, K. L., Bacon, K. D., Sheppard, B. C., Ashktorab, H., Smooth, D. T., Cover, T. L., Deveney, C. W., and Rutten, M. J. (2003) *Am. J. Physiol.* **285**, G163–G176
32. Takahashi, A., Camacho, P., Lechleiter, J. D., and Herman, B. (1999) *Physiol. Rev.* **79**, 1089–1125
33. Hasson, L. E., Nyren, O., Hsing, A. W., Bergstrom, R., Josefsson, S., Chow, W. H., Fraumeni, J. F., Jr., and Adami, H. O. (1996) *N. Engl. J. Med.* **335**, 242–249
34. Yao, X., Anderson, K. L., and Cleveland, D. W. (1997) *J. Cell Biol.* **139**, 435–447
35. Uemura, N., Okamoto, S., Yamamoto, S., Matsumura, N., Yamaguchi, S., Yamakido, M., Taniyama, K., Sasaki, N., and Schlemper, R. J. (2001) *N. Engl. J. Med.* **345**, 784–789
36. Marlink, K. L., Bacon, K. D., Sheppard, B. C., Ashktorab, H., Smoot, D. T., Cover, T. L., Deveney, C. W., and Rutten, M. J. (2003) *Am. J. Physiol.* **285**, G163–G176
37. Yao, X., and Forte, J. G. (1994) in *Molecular and Cellular Mechanisms of H⁺ Transport* (Hirst, B. H., ed) Springer, Heidelberg
38. Wang, K. K. W. (1999) in *Calpain: Pharmacology and Toxicology of Calcium-dependent Protease* (Wang, K. K. W., and Yuen, P. W., eds) pp. 77–102, Taylor & Francis, Philadelphia
39. Necchi, V., Candusso, M. E., Tava, F., Luinetti, O., Ventura, U., Fiocca, R., Ricci, V., and Solcia, E. (2007) *Gastroenterology* **132**, 1009–1023
40. Black, J. A., Forte, T. M., and Forte, J. G. (1981) *Gastroenterology* **81**, 509–519
41. Zhou, R., Zhu, L., Kodani, A., Hauser, P., Yao, X., and Forte, J. G. (2005) *J. Cell Sci.* **118**, 4381–4391
42. Tamura, A., Kikuchi, S., Hata, M., Katsuno, T., Matsui, T., Hayashi, H., Suzuki, Y., Noda, T., Tsukita, S., and Tsukita, S. (2005) *J. Cell Biol.* **169**, 21–28
43. Gauthier, N. C., Monzo, P., Kaddai, P., Doye, A., Ricci, V., and Boquet, P. (2005) *Mol. Biol. Cell* **16**, 4852–4866
44. El-Omar, E. M., Penman, I. D., Ardill, J. E., Chittajallu, R. S., Howie, C., and McColl, K. E. (1995) *Gastroenterology* **109**, 681–691